

Designing multilayer dielectric filter based on TiO₂/SiO₂ for fluorescence microscopy applications

Hanh Hong Mai¹

¹ Faculty of Physics, VNU University of Science,
334 Nguyen Trai, Hanoi, Vietnam

Abstract

This study presents a new construction design of a distributed Bragg reflector (DBR) filter and a Fabry–Pérot (FP) filter by using needle technique as a synthesis method. The optimized DBR and FP filters having a proper number of layers with controlling thickness TiO₂/SiO₂ are utilized to transmit only a certain narrow band of wavelengths while blocking the others. As a proof of concept, the filters are designed to selectively transmit only a very narrow band of wavelength at 780 nm which is the near infrared (NIR) fluorescent emission from Alexa Fluor 750 dye. The obtained results show that the optimized filters represent advanced spectral performance which can be used to improve the sensitivity and the imaging contrast in fluorescence microscopy.

Keywords: Bragg reflectors, DBR filter, Fabry–Pérot, Fabry–Pérot filter, thin film, thin film deposition, Needle method.

Citation: Mai HH. Designing multilayer dielectric filter based on TiO₂/SiO₂ for fluorescence microscopy applications. *Computer Optics* 2020; 44(2): 209-213. DOI: 10.18287/2412-6179-CO-618.

Acknowledgement: This research was supported by the International Centre for Genetic Engineering and Biotechnology (ICGEB) through a grant to Dr. Hanh Hong Mai. Grant NO. CRP/VNM17-03.

Introduction

Fluorescent dyes are frequently used as cell and tissue labels in fluorescence microscopy and cell biology [1–3]. They can be conjugated to a variety of antibodies, streptavidin, peptides, proteins, tracers, and amplification substrates [4]. In fluorescence microscopy imaging, after conjugating onto biological specimens, they can emit a wide range of wavelength spanning from visible (VIS) to near infrared (NIR) under a continuous illumination of a light source, thus, generates images [5–8]. In common fluorescence microscopes, the detectors normally present better sensitivity in VIS range than in the NIR range. As a result, the fluorescent intensities detected in NIR range are lower than that in VIS range. Very often, they are even lower than the reflected, scatter or even diffracted light from excitation light sources. Thus, the images obtained from specimens conjugated with NIR dyes are normally dimmer with lower imaging contrast compared to specimens conjugated with VIS dyes. Technically speaking, the image contrast can be improved by allowing only NIR emission to reach to the detector while blocking other emissions. This can be done in a fluorescence microscope by implementing band-pass filters which allow only NIR light to transmit while filtering out others.

Band-pass filters based on thin film technology has been attracted a lot of attention in microscopy imaging [9–11]. They consist of alternating layers of high and low refractive index materials with particular thicknesses. They function based on the principle of multiple reflections and interferences between high and low index material interfaces [10, 12]. Technically speaking, the performance of band-pass filters can be altered by changing the character-

istic of the component films i.e. refractive index of layers and optical thicknesses [12–15]. DBR filter is a type of band-pass filters. In order to satisfy the interfering condition, their layers are defined as quarter-wave thick of the center wavelength. A DBR filter normally exhibits a very high reflectivity in a certain range of wavelengths around a center wavelength. This high reflection region is known as the DBR stopband, and is governed by the refractive index contrast between the constituent layers [9, 12, 13]. The higher the refractive index contrast, the broader the stopband is obtained. A Fabry–Pérot (FP) filter, on the other hand, consists of a cavity between two highly reflecting DBR filters. By inserting a half wavelength cavity, a very narrow band of a designed wavelength can be highly transmitted within the stopband [14–19].

Taking advantages of band-pass filters based on thin film technology, in this work, an optimal design of DBR and FP filters based on needle technique which can transmit only a narrow band in NIR range while blocking others will be introduced. The filters are based on a stack of TiO₂/SiO₂ which are vital dielectric materials with wide band-gap energies and high refractive index contrast [9, 20–22]. TiO₂ is selected for high refractive index layer of 2.5 and SiO₂ as a low refractive index layer of 1.45. As a proof of concept, a combination of an optimized DBR and a FP filters was designed with a central wavelength of 780 nm to selectively transmit a narrow band of wavelength at 780 nm emitted from a NIR fluorescent Alexa Fluor 750 dye while blocking the others [3]. Additionally, in order to clarify the accuracy of the optimal filter designs, comparisons between the initial and optimized filter spectrum, and between optimized and experimental filter spectrum are also taken into account.

1. Theoretical basis

Consider a band-pass filter surrounded by an environment. Light from the source falls on the filter at an angle ϑ_0 , and a wave front penetrates the filter surface can be considered as planar. To calculate the transmission and reflection spectra of a multilayer band-pass filter, transfer matrix method is normally applied. Herein, a band pass filter consisting of q thin film layers is represented as a system matrix which is the product of the individual layer matrices, taken in the correct order, given by [9]:

$$\begin{bmatrix} B \\ C \end{bmatrix} = \left\{ \prod_{r=1}^q \begin{bmatrix} \cos \delta_r & (i \sin \delta_r) / n_r \\ in_r \sin \delta_r & \cos \delta_r \end{bmatrix} \right\} \begin{bmatrix} 1 \\ \eta_m \end{bmatrix},$$

where, B and C are the normalized electric and magnetic fields at the front interface

$$\delta_r = 2\pi n_r d_r \cos \vartheta_r / \lambda ;$$

n_r is the refractive index of layer, d_r is the physical thickness layer, q is the number of layers next to substrate, ϑ_r is the reflected angle which can be derived from an incident angle ϑ_0 by Snell's law. η_m is the substrate admittance.

The expression for transmittance of a multilayer system which is defined as the ratio of the output intensity from thin film assembly to input intensity, is given as follow: The system matrix finally will be converted back into reflection and transmission spectra.

$$R = \left(\frac{\eta_0 B - C}{\eta_0 B + C} \right) \left(\frac{\eta_0 B - C}{\eta_0 B + C} \right)^*,$$

$$T = \frac{4n_0 \operatorname{Re}(n_s)}{(\eta_0 B - C)(\eta_0 B + C)},$$

η_0 is the incident medium of admittance, n_s is the refractive index of the substrate, and $\operatorname{Re}(n_s)$ represents the real part of refractive index of substrate. Based on the transfer matrix method a reflection spectrum and transmission spectrum of a DBR and a FP filter are calculated and presented in Fig. 1 and Fig. 2. Here, a spectrum region where the DBR and the FP filter provide extremely high reflectance is the stopband. Within a stopband, a sharp, high intensity peak denoting high transmission of a very narrow band of wavelengths appears. It is generated from the half wavelength cavity in between the two DBRs of a FP filter.

2. Optimization of multilayer filters

It is often difficult, or even impossible, to manually design a filter respecting all the requirements for a given application. However, it is possible to optimize a filter using synthesis methods. The most commonly used synthesis method is the needle method [9, 10, 23]. The needle method was first described by Tikhonravov in 1982 [24]. The essence of needle technique is that using an algorithm to identify convenient places to insert new layers that will improve the discrepancy between the target and solution which is well known as merit function.

Technically speaking, the optimal position of needle to be added is where derivative of merit function is negative. Mostly a few single needle layers are added and transmission/reflection spectrum is calculated. The addition of needle layers stops at the point where there is no improvement in the target transmission/reflection spectrum.

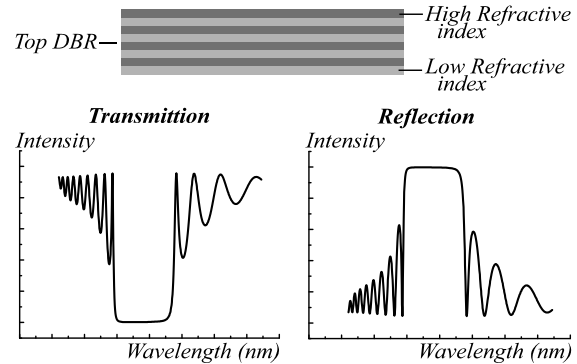


Fig. 1. Reflection spectrum and transmission spectrum of a DBR filter

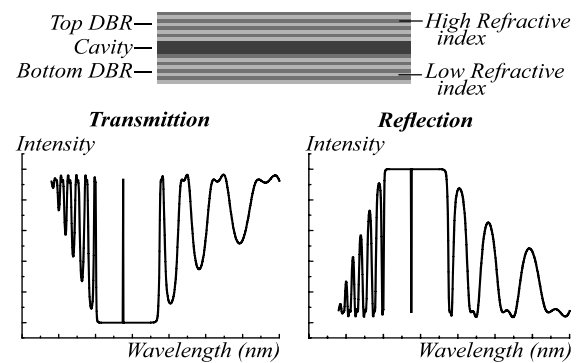


Fig. 2. Reflection and transmission spectrum of a FP filter consisting of a cavity and two DBRs

3. Requirements of designed filters

In this work, the proposed filters are utilized to improve the sensitivity and imaging contrast in fluorescence microscopy. An example of a fluorescence microscopy is shown in Fig. 3. It consists of a light source, biological specimens conjugated with different dyes including Alexa Fluor 750 dye, a FP filter and a detector. In common fluorescence microscopes, the light source is a Halogen lamp which covers a broad range of wavelength from UV to NIR range (from 200 nm to 2000 nm). The detector, on the other hand, normally covers a shorter range of wavelength from 250 nm to 1000 nm. Its sensitivity in NIR range (from 750 nm to 1000 nm) is very poor compared to that in VIS range. The working range (stopband) of a FP filter is shortest which is normally less than 300 nm. That means unwanted wavelengths coming from outer side of the stopband can also reach to the detector, causes poor imaging contrast and low sensitivity. Therefore, filtering out the wavelengths outside the filter stopband is always of high demand.

In order to improve the sensitivity and image contrast in NIR range, one solution is to include a compact of optimal DBR and FP filters in the setup to allow only a very

narrow NIR band of a specific wavelength to pass through. The proposed exemplary fluorescence microscopy is demonstrated in Fig. 4. An optimized DBR and a FP filter will be implemented in the setup to allow only the wavelength of 780 nm to transmit, thus, reaching to the detector, while blocking other wavelengths outside the stopband. Additionally, the transmitted peak is required to have high intensity while still exhibiting a narrow peak width (FWHM).

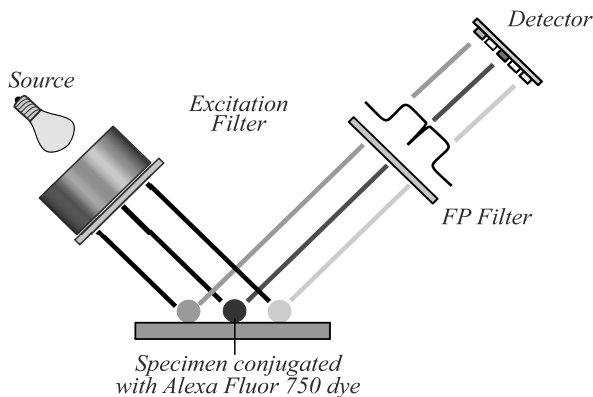


Fig. 3. An exemplary fluorescence microscopy. It consists of a light source, a FP filter and a detector. Wavelengths outside the stopband are also detected in this setup

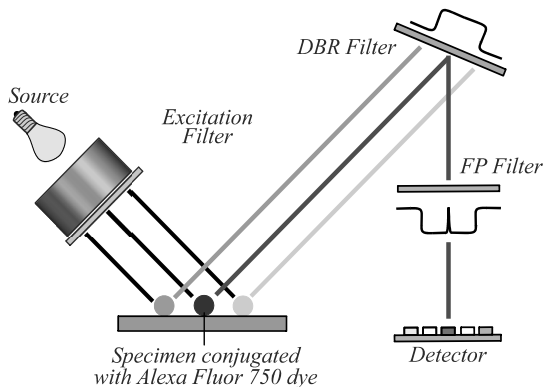


Fig. 4. A proposed exemplary fluorescence microscopy. An optimized DBR and a FP filter are included in the setup to only transmit 780 nm while blocking the wavelengths outside the stopband

4. Optimization designs and discussion

In this work, the open-source software, Open Filters, and its needle function are used to optimize the designs of DBR and FP filters based TiO₂/SiO₂ [23, 25]. To decrease the stimulation time, an initial DBR design close to the required design can be synthesized using H(LH)^{*p*} layer configuration [11, 16, 20, 26, 27], where H and L are quarter-wave thick of high and low refractive index layers and *p* is the number of repeated high and low refractive index pairs. Similarly, an initial FP filter design with layer structure of H(LH)^{*q*} 2L H(LH)^{*q*} was chosen, in which H(LH)^{*q*} represents the top and the bottom DBR, 2L describes a half wavelength cavity. The repeated high and low refractive index pairs *q* in this design is 4. The center wavelength in both cases is 780 nm.

In this case, the high refractive index is denoted for TiO₂, and low refractive index is denoted for SiO₂. *p* in this case is chosen to be 10. The angle of the incident light was chosen as 0° degrees. Note that, the transmitted and reflected light in all cases were selected as unpolarized light.

The DBR reflection spectrum of the initial design is presented in Fig. 5 showing in a stopband of 225 nm (from 675 nm to 900 nm) with high reflectivity of almost 0.97 and two sharp edges. However, there are fringes with high reflectivity outside the stopband. That means the DBR filter not only reflect the wavelength range inside but also outside the stopband. The reflected light outside the stopband will cause noise signal, which create a significant impact on the low sensitivity and low contrast of microscopy imaging. By using needle function, an optimized DBR filter design with 26 layers and total thickness of 2340 nm was obtained. Compared to the initial design, the optimized DBR filter still maintains high reflectivity within the stopband, remains the stopband width of 225 nm, however, the fringes outside the stopband are significantly suppressed. The data of the optimized DBR filter design is presented in Table 1.

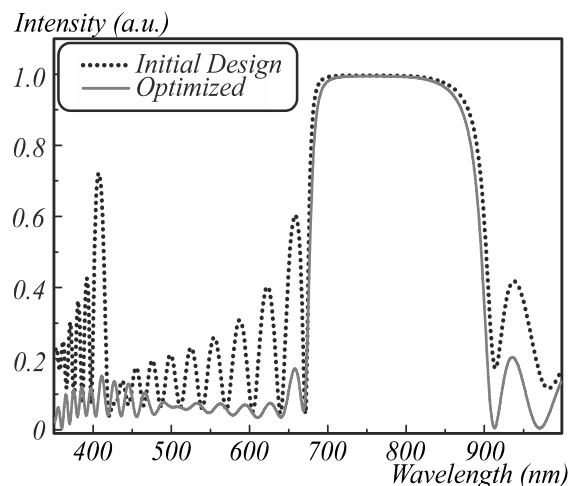


Fig. 5. Reflection spectra of an initial and an optimized design of a DBR filter

Fig. 6 represents the FP transmission spectrum of the initial design, showing in a stopband of 250 nm and a sharp, high intensity peak (narrow band of wavelength) at 780 nm. However, outside the stopband there are fringes with fluctuated transmission intensity. By using needle function, an optimized FP filter design with 22 layers and total thickness of 2144 nm was obtained. Compared to the initial design, a small shift to shorter wavelength of 30 nm is observed. However, the stopband width is maintained 250 nm. Most importantly, the transmission peak remains a high intensity at 780 nm. This allows the fluorescent emission of Alexa Fluor 750 dye can be transmitted thoroughly the DBR and the FP without attenuation. Similar to the previous case, the fringes outside the stopband is significantly suppressed. The data of the optimized DBR filter design is presented in Table 2.

In order to verify the optical quality and the accuracy of the optimized filters, a comparison between the simulated and experimental transmission spectra of an optimized DBR filter is taken into account. To simplify the deposition process, an optimized filter with only 13 layers of TiO₂/SiO₂ is considered. Based on the thickness data of the optimized design, a DBR filter was deposited by using vacuum coating systems (Univex 400). Comparing simulated data and experimental data, good correlations in the

stopband position and stopband width are observed (Fig. 7). Similar to the simulated spectrum, the experimental spectrum also exhibits negligible fringes outside of the stopband. A small shift to longer wavelength of the stopband is most likely caused by variation of the real layer thicknesses. Furthermore, an increase in reflection (equivalent to a decrease in transmission) at the edge of the stopband (at wavelength of 950 nm) is also observed. It is due to the high absorbance of TiO₂ in NIR range [28].

Table 1. Layer thickness of TiO₂/SiO₂ based DBR filter with a central wavelength of 780 nm

Layer No.	Material	Thickness (nm)	Layer No.	Material	Thickness (nm)
1	TiO ₂	90.25	14	SiO ₂	135.87
2	SiO ₂	146.13	15	TiO ₂	81.65
3	TiO ₂	82.52	16	SiO ₂	138.04
4	SiO ₂	134.21	17	TiO ₂	84.05
5	TiO ₂	80.36	18	SiO ₂	147.95
6	SiO ₂	134.95	19	TiO ₂	15.30
7	TiO ₂	80.02	20	SiO ₂	30.11
8	SiO ₂	134.89	21	TiO ₂	14.46
9	TiO ₂	80.77	22	SiO ₂	144.88
10	SiO ₂	135.12	23	TiO ₂	75.39
11	TiO ₂	81.04	24	SiO ₂	10.74
12	SiO ₂	135.33	25	TiO ₂	7.36
13	TiO ₂	81.47	26	SiO ₂	57.47

Table 2. Layer thickness of TiO₂/SiO₂ based FP filter with a central wavelength of 780 nm

Layer No.	Material	Thickness (nm)	Layer No.	Material	Thickness (nm)
1	TiO ₂	77.95	12	SiO ₂	18.49
2	SiO ₂	138.73	13	TiO ₂	73.34
3	TiO ₂	75.86	14	SiO ₂	133.07
4	SiO ₂	129.57	15	TiO ₂	71.73
5	TiO ₂	73.79	16	SiO ₂	129.47
6	SiO ₂	128.23	17	TiO ₂	73.79
7	TiO ₂	68.95	18	SiO ₂	130.95
8	SiO ₂	133.26	19	TiO ₂	73.27
9	TiO ₂	78.68	20	SiO ₂	131.28
10	SiO ₂	262.87	21	TiO ₂	68.29
11	TiO ₂	10.07	22	SiO ₂	62.08

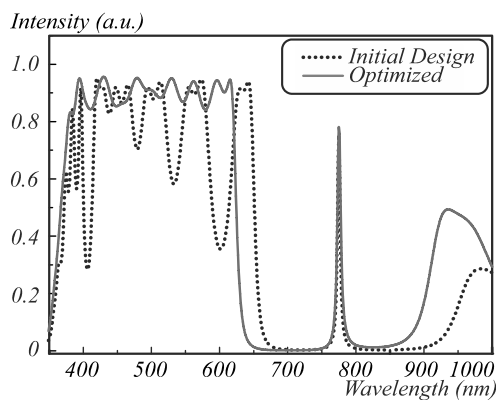


Fig. 6. Transmission spectra of an initial and an optimized design of a FP filter

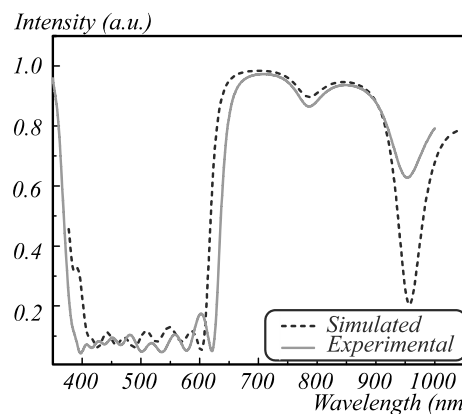


Fig. 7. Simulated and experimental reflection spectra of an optimized DBR filter with 13 layers

Conclusion

In this work DBR and FP filters are designed and optimized to transmit the NIR fluorescent emission at 780 nm from Alexa Fluor 750 dye conjugated onto biological specimens while blocking other wavelengths. It has been shown that the optimized filters still maintain

the most important characteristic properties of initial filter designs such as high reflectivity within the stopband, remaining stopband width, and high transmission at the 780 nm peak. Furthermore, by using needle technique, the fringes outside the stopband is significantly suppressed which helps to block all other wavelengths outside the stopband. The simulated reflection spectrum of

an optimized DBR filter design containing 13 layers of TiO₂/SiO₂ show a good correlation with experimental spectrum. The obtained results can be considered as an important base for the applications of optimized DBR and FP filters in microscopy imaging.

References

- [1] Matsunaga T, Okochi M, Nakasono S. Direct count of bacteria using fluorescent dyes: Application to assessment of electrochemical disinfection. *Anal Chem* 1995; 67: 4487-4490. DOI: 10.1021/ac00120a010.
- [2] Yuan L, Lin W, Yang Y, Chen H. A unique class of near-infrared functional fluorescent dyes with carboxylic-acid-modulated fluorescence ON/OFF switching: Rational design, synthesis, optical properties, theoretical calculations, and applications for fluorescence imaging in living animals. *J Am Chem Soc* 2012; 134: 1200-1211. DOI: 10.1021/ja209292b.
- [3] Invitrogen. Alexa fluor[®] dyes: Simply the best and brightest fluorescent dyes and conjugates. *Molecular Probes Inc*; 2005: 1-36.
- [4] Oliveira E, Bértolo E, Núñez C, Pilla V, Santos HM, Fernández-Lodeiro J, et al. Green and red fluorescent dyes for translational applications in imaging and sensing analytes: A dual-color flag. *ChemistryOpen* 2018; 7(1): 9-52. DOI: 10.1002/open.201700135.
- [5] Young MR. Principles and technique of fluorescence microscopy. *J Cell Sci* 1961; s3-102: 419-449.
- [6] Drummen GPC. Fluorescent probes and fluorescence (microscopy) techniques – Illuminating biological and biomedical research. *Molecules* 2012; 17: 14067-14090. DOI: 10.3390/molecules171214067.
- [7] Ettinger A, Wittmann T. Fluorescence live cell imaging. In *Book: Waters JC, Wittman T, eds. Quantitative imaging in cell biology. Vol. 123. Ch 5. Academic Press; 2014: 77-94.* DOI: 10.1016/B978-0-12-420138-5.00005-7.
- [8] Thorn K, Kellogg D. A quick guide to light microscopy in cell biology. *Mol Biol Cell* 2016; 27: 219-222. DOI: 10.1091/mbc.e15-02-0088.
- [9] MacLeod HA. Thin-film optical filters. 4th ed. Taylor & Francis Book; 2010. ISBN: 978-1-4200-7302-7.
- [10] Marthinsen H. Numerical methods for optical interference filters. *Norwegian University of Science and Technology*; 2009.
- [11] Habib M, Ullah A. Simulation of near Infrared interference bandpass filters for spectroscopic applications. 2016 International Conference on Computing, Electronic and Electrical Engineering (ICECUBE) 2016: 234-238. DOI: 10.1109/ICECUBE.2016.7495230.
- [12] Nazar A, Ali AH, Jasem NA. New construction stacks for optimization designs of edge filter. *IOSR J Appl Phys* 2016; 8(3-II): 20-26. DOI: 10.9790/4861-0803022026.
- [13] Nazar A. Design optical filters using two different synthesis approaches. *Journal of Kufa – physics* 2011; 3(1): 45-58.
- [14] de Denus-Baillargeon M-M, Abel-Tibérini L, Lequime M, Carignan C, Épinat B, Gach J-L, et al. Developing high-performance reflective coatings for the tunable filter and the high-order interferometer of the 3D-NTT. *Soc Photo Optical Instrum Eng Conf Ser* 2008; 7013: 111. DOI: 10.1117/12.789498.
- [15] Butt MA, Fomchenkov SA, Khonina SN. Dielectric-Metal-Dielectric (D-M-D) infrared (IR) heat reflectors. *J Phys Conf Ser* 2017; 917: 62007. DOI: 10.1088/1742-6596/917/6/062007.
- [16] de Denus-Baillargeon M-M, Schmitt T, Larouche S, Martinu L. Design and fabrication of stress-compensated optical coatings: Fabry–Perot filters for astronomical applications. *Appl Opt* 2014; 53(12): 2616-2624. DOI: 10.1364/AO.53.002616.
- [17] Butt MA, Strelkov YuS. An approach to developing a Fabry-Perot filter by a single fabrication step for gas sensing applications. *Proc SPIE* 2018; 10774: 107740P. DOI: 10.1117/12.2316482.
- [18] Butt MA, Khonina SN, Kazanskiy NL. Numerical analysis of a miniaturized design of a Fabry–Perot resonator based on silicon strip and slot waveguides for bio-sensing applications. *J Mod Opt* 2019; 66(11): 1172-1178. DOI: 10.1080/09500340.2019.1609613.
- [19] Butt MA, Khonina SN, Kazanskiy NL. Label-free detection of ambient refractive index based on plasmonic Bragg gratings embedded resonator cavity sensor. *J Mod Opt* 2019; 66(19): 1920-1925. DOI: 10.1080/09500340.2019.1683633.
- [20] Butt MA, Fomchenkov SA, Ullah A, Habib M, Ali RZ. Modelling of multilayer dielectric filters based on TiO₂/SiO₂ and TiO₂/MgF₂ for fluorescence microscopy imaging. *Computer Optics* 2016; 40(5): 674-678. DOI: 10.18287/2412-6179-2016-40-5-674-678.
- [21] Butt MA, Fomchenkov SA, Ullah A, Verma P, Khonina SN. Biomedical bandpass filter for fluorescence microscopy imaging based on TiO₂/SiO₂ and TiO₂/MgF₂ dielectric multilayers. *J Phys Conf Ser* 2016; 741: 012136. DOI: 10.1088/1742-6596/741/1/012136.
- [22] Butt MA, Fomchenkov SA, Khonina SN. Multilayer dielectric stack notch filter for 450-700 nm wavelength spectrum. *CEUR Workshop Proceedings* 2017; 1900: 1-4. DOI: 10.18287/1613-0073-2017-1900-1-4.
- [23] Nazar A. Open Filters: For optimum design wideband ARC's at oblique incidence of light and effect dispersion of material coating. *Journal of College of Education* 2012; 2: 760-773.
- [24] Tikhonravov AV, Trubetskov MK, DeBell GW. Application of the needle optimization technique to the design of optical coatings. *Appl Opt* 1996; 35: 5493-5508. DOI: 10.1364/AO.35.005493.
- [25] Larouche S, Martinu L. OpenFilters: open-source software for the design, optimization, and synthesis of optical filters. *Appl Opt* 2008; 47: C219. DOI: 10.1364/AO.47.00C219.
- [26] Tang H, Gao J, Zhang J, Wang X, Fu X. Preparation and spectrum characterization of a high quality linear variable filter. *Coatings* 2018; 8: 308. DOI: 10.3390/coatings8090308.
- [27] Jen Y-J, Lin M-J. Design and fabrication of a narrow bandpass filter with low dependence on angle of incidence. *Coatings* 2018; 8: 231. DOI: 10.3390/coatings8070231.
- [28] Sta I, Jlassi M, Hajji M, Boujmil MF, Jerbi R, Kandyla M, et al. Structural and optical properties of TiO₂ thin films prepared by spin coating. *J Sol-Gel Sci Technol* 2014; 72(2): 421-427. DOI: 10.1007/s10971-014-3452-z.

Author's information

Hanh Hong Mai (b. 1984) is a lecturer at Quantum Optics Department, Physics Faculty, VNU University of Science, Hanoi, Vietnam. She holds a PhD in Engineering from the University of Kassel, Germany (2012). She attained her Master's degree in Optics from VNU University of Science (2008). Prior to this, she received her Bachelor degree in Optics from VNU University of Science. In 2013, she made a research stay at Physics and Astronomy Department, KU Leuven, Belgium. Her current research topics are fluorescent sensors, micro lasers based biomaterials, and smartphone based devices for bio-medical applications. E-mail: hanhhongmai@hus.edu.vn. ORCID ID: 0000-0002-5924-5112/

Received August 13, 2019. The final version – January 14, 2020.